Accepted Manuscript

Silver nanoparticles enhance wound healing in zebrafish (*Danio rerio*)

Seung Beom Seo, S.H.S. Dananjaya, Chamilani Nikapitiya, Bae Keun Park, Ravi Gooneratne, Tae-Yoon Kim, Jehee Lee, Cheol-Hee Kim, Mahanama De Zoysa

PII: S1050-4648(17)30451-5

DOI: 10.1016/j.fsi.2017.07.057

Reference: YFSIM 4739

To appear in: *Fish and Shellfish Immunology*

Received Date: 9 March 2017

Revised Date: 17 July 2017

Accepted Date: 26 July 2017

Please cite this article as: Seo SB, Dananjaya SHS, Nikapitiya C, Park BK, Gooneratne R, Kim T-Y, Lee J, Kim C-H, De Zoysa M, Silver nanoparticles enhance wound healing in zebrafish (*Danio rerio*), *Fish and Shellfish Immunology* (2017), doi: 10.1016/j.fsi.2017.07.057.

Silver nanoparticles enhance wound healing in zebrafish (*Danio rerio*)

Seung Beom Seo [a †], S.H.S. Dananjaya [a †], Chamilani Nikapitiya [b, c], Bae Keun Park [a], Ravi Gooneratne [d], Tae-Yoon Kim[e], Jehee Lee [b, c], Cheol-Hee Kim [e*], Mahanama De Zoysa [a, c **]

[a] *College of Veterinary Medicine and Research Institute of Veterinary Medicine, Chungnam National University, Yuseong-gu, Daejeon, 34134, Republic of Korea*

[b] *Department of Marine Life Sciences, School of Marine Biomedical Sciences, Jeju National University, Jeju Self-Governing Province, 63243, Republic of Korea*

[c] *Fish Vaccine Research Center, Jeju National University, Jeju Self-Governing Province, 63243, Republic of Korea*

[d] *Centre for Food Research and Innovation, Department of Wine, Food and Molecular Biosciences, Faculty of Agriculture & Life Sciences, Lincoln University, New Zealand*

[e] *Department of Biology, Chungnam National University, Yuseong-gu, Daejeon, 34134, Republic of Korea*

[†] These authors contributed equally to this study.

Corresponding authors:

[*]Cheol-Hee Kim

Department of Biology, Chungnam National University, Yuseong-gu, Daejeon, 34134, Republic of Korea

E-mail address: zebrakim@cnu.ac.kr (C.H. Kim).

[**]Mahanama De Zoysa

College of Veterinary Medicine and Research Institute of Veterinary Medicine, Chungnam National University, Yuseong-gu, Daejeon 34134, Republic of Korea

E-mail address: mahanama@cnu.ac.kr (M. De Zoysa).

Graphical Abstract

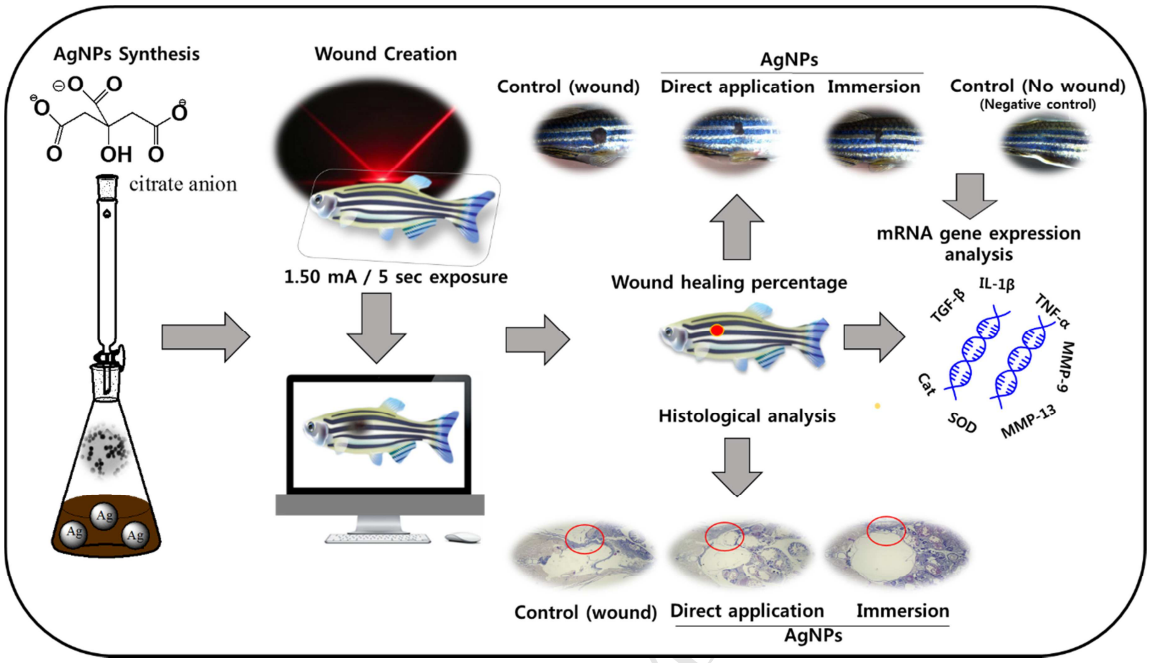

ABSTRACT

Silver nanoparticles (AgNPs) were successfully synthesized by a chemical reduction method, physico-chemically characterized and their effect on wound-healing activity in zebrafish was investigated. The prepared AgNPs were circular-shaped, water soluble with average diameter and zeta potential of 72.66 nm and −0.45 mv, respectively. Following the creation of a laser skin wound on zebrafish, the effect of AgNPs on wound-healing activity was tested by two methods, direct skin application (2 µg/wound) and immersion in a solution of AgNPs and water (50 µg/L). The zebrafish were followed for 20 days post-wounding (dpw) by visual observation of wound size, calculating wound healing percentage (WHP), and histological examination. Visually, both direct skin application and immersion AgNPs treatments displayed clear and faster wound closure at 5, 10 and 20 dpw compared to the controls, which was confirmed by 5 dpw histology data. At 5 dpw, WHP was highest in the AgNPs immersion group (36.6%) > AgNPs direct application group (23.7%) > controls (18.2%), showing that WHP was most effective in fish immersed in AgNPs solution. In general, exposure to AgNPs induced gene expression of selected wound-healing-related genes, namely, transforming growth factor (TGF-β), matrix metalloproteinase (MMP) -9 and -13, pro-inflammatory cytokines (IL-1β and TNF-α) and antioxidant enzymes (superoxide dismutase and catalase), which observed differentiation at 12 and 24 h against the control; but the results were not consistently significant, and many either reached basal levels or were down regulated at 5 dpw in the wounded muscle. These results suggest that AgNPs are effective in acceleration of wound healing and altered the expression of some wound-healing-related genes. However, the detailed mechanism of enhanced wound healing remains to be investigated in fish.

Keywords: Silver nanoparticles, Inflammation, Gene expression, Zebrafish, Wound healing

1. Introduction

Aquatic organisms are impacted by a wide range of factors including environmental conditions (ocean acidification), mechanical and physical injuries (aggressive interaction, stocking density, abrasion from nets and cages, fish sorting, transportation), pollutants (metal ions, pesticides, industrial discharges) and diseases that can cause tissue damage, increased apoptosis, necrosis and even death [1–8]. Many infective agents affect fish skin and muscle structure, and consequently the quality and survival of fish [9–11]. When skin and tissue damage occur, a rapid wound healing process is essential to prevent entry of pathogens and secondary infections.

Wound healing and tissue repair is an essential and complex process that ensures the health and survival of organisms, and impaired wound healing can lead to difficulties in treating deep tissue infections [12–15]. Wound healing consists of three overlapping phases: hemostasis/inflammation, proliferation and remodeling [14]. Each of these phases involves the co-ordination of different cell types, complex signaling networks, activity of various growth factors and inflammatory mediators, extracellular matrix (ECM) synthesis and degradation [16,17]. Although various wound healing agents are widely used, it has recently been shown that topical drug delivery systems based on certain nanoparticles (NPs) are effective for transporting antibiotics into deep tissues [18,19]. Nanotechnology is already being used in the aquaculture industry in a variety of processes [20] and opportunities exist for a nanotechnology-based biomedical approach to improve the health of aquatic animals. For example NP-based agents could be developed to act as immunostimulants, antimicrobial agents for drug delivery and for wound healing. Thus, there is a continuous demand for research into utilizing metallic NPs and biodegradable polymers [20, 21] as therapeutic agents for efficient controlling of infectious

diseases in aquaculture. Among the different NP materials, silver-based materials (AgNPs) have long been used as bactericidal agents and at present they are being used in household appliances and consumer goods, including wound dressings [22]. Although the antimicrobial [23–25] and anti-inflammatory [26] properties of AgNPs are well recognized, safety issues are raised about the use of AgNPs in human and aquatic systems due to unintentional health and environmental impacts [27–29]. To our knowledge an AgNPs-based wound healing approach in aquaculture has not been extensively reported. However, in a report of AgNPs and the freshwater fish *Anabas testudineus*, it was shown that the application of AgNPs to an open wound induced significant wound contraction and accelerated wound closure and healing time [30].

In the present study, the zebrafish was used as the model to investigate the effect of AgNPs on wound healing. AgNPs were synthesized and two methods of AgNPs administration were tested in zebrafish wounded by a laser beam. Wound healing efficacy was evaluated by comparing wound contraction changes (wound closure) visually, calculating wound healing percentage (WHP) and by histological examination of the wounded and recovering tissue. Since knowledge of the cellular and molecular mechanisms involved in the healing processes related to AgNPs-treated wounds in fish is still limited, this study was extended to investigate gene expression involved in different phases of wound healing at12 and 24 h and 5 days post-wounding (dpw).

2. Materials and methods

2.1. Synthesis of AgNPs

The AgNPs were prepared using a chemical reduction method [31]. In brief, 0.36 g of $AgNO_3$ (Sigma, Aldrich) was dissolved in 5 mL of deionized water in a beaker. Separately,

flocculate was prepared by mixing 2.5 mL of 1.08 M ferrous sulfate heptahydrate ($FeSO_4.7\ H_2O$) and 3.5 mL of 1.37 M trisodium citrate dehydrate ($C_6H_5Na_3O_5$) (Sigma, Aldrich). Then, 6 mL of flocculate was added to the $AgNO_3$ solution dropwise while it was mixed vigorously by magnetic stirrer for 8 min. The resultant opaque brown-black AgNPs suspension was centrifuged at 3500 rpm for 10 min, the supernatant discarded and the black-blue pellet re-suspended in 10 mL of 0.68 M $C_6H_5Na_3O_5$. This step was repeated minimum of five times to produce a pure AgNPs pellet which was dissolved in water and used for the physiochemical characterization and wound-healing experiments in zebrafish.

2.2. Characterization of AgNPs

The synthesized AgNPs were thoroughly characterized by several physiochemical techniques. The UV-vis absorbance spectrum was determined using a spectrophotometer (Mecasys, Republic of Korea), operating in the absorbance mode, scanned in the wavelength range 250–600 nm with water as the reference. The morphology of the AgNPs was observed using a field emission scanning electron microscope (FE-SEM) (Model S-4800, Hitachi, Japan) after coating with platinum by ion sputter (E-1030, Hitachi, Japan). One drop of the AgNPs solution was allowed to evaporate at room temperature on a 200-mesh copper grid, covered by a carbon support film (CF200-Cu, Electron microscopy science, UK) prior to examination under a field emission transmission electron microscope (FE-TEM) (Technai G2 F30 S-Twin, FEI, USA). The average particle size distribution and zeta potential of the AgNPs were measured using Zetasizer S-90 Malvern instruments (Malvern, UK).

2.3. Zebrafish culture

Wild-type zebrafish were obtained from a commercial aquarium in Seoul, Republic of Korea. Fish were maintained in standard laboratory conditions at 28 ±1 °C with 12 h light/12 h dark cycles in an automated water circulation system (10 fish/3.5 L tank). Fish were fed with brine shrimp (artemia) thrice daily at 4% of body weight. Healthy uniform-size fish (4 months old) were chosen for the experiments. All experiments related to zebrafish were conducted accordance with the institutional animal care guidelines and supervision of committees of Chungnam National University (CNU-00927).

2.4. Determination of AgNPs toxicity to zebrafish

To determine the toxicity of the AgNPs, zebrafish were immersed in different AgNPs concentrations (0, 25, 50, 100, 200 and 400 µg/L) in six tanks (10 fish/tank). Fish mortality was noted at 6, 12, 24, 48, 72 and 96 h post-immersion (hpi). Fish deaths (%) were plotted against the AgNP concentrations and toxicity expressed as the 50% lethal dose of toxicity (LD_{50}), the concentration at which 50% of fish death occurred relative to non-exposed control fish.

2.5. Laser-based wounding and AgNPs treatment

To determine the wound healing percentage, the zebrafish were divided into three groups of 12 (n = 36). All fish were anaesthetized by immersion in 0.2% Tricaine (ethyl 3-aminobenzoate methane-sulfonate) (Sigma, Aldrich). Following anesthesia, a single wound was created with a laser beam (150 mA for 5 sec), posterior to the gill area, close to the lateral line of the zebrafish (Fig. 1). To test the AgNPs effects on wound-healing activity in zebrafish, to the first group (under anesthesia), 2 µg of AgNPs were directly applied to the wound site on the day of wounding (0 dpw) and on 2, 5 and 7 dpw. The fish were kept for 4 min outside of the tank

following on each application day and then transferred to temporary recovery tank containing water for 5 min to get rid of excess AgNPs on the wound, before being returned to the experimental tank of direct application. The second group of wounded fish were immersed into an AgNPs-water (50 µg/L) solution, also kept outside for 4 min on 0, 2, 5 and 7 dpw, and the AgNPs tank water changed on 2, 5 and 7 dpw to simulate group 1 reapplication conditions. Similarly, the third group, the control (wounded-untreated) fish, was also kept outside for 4 min, and the plain water changed on 2, 5 and 7 dpw to simulate group 1 and 2 conditions. For histological analysis a separate experiment was conducted with the same experimental design as above. Muscle tissues at the wounded site were collected from three fish per group (wounded untreated, direct application and immersed) at each of six time points (n = 54 fish).

2.6. Effect of AgNPs on wound healing

2.6.1. Visual observation and wound healing percentage (WHP)

On 2, 5, 10 and 20 dpw, when zebrafish were under anesthesia, the wounds of 12 fish per group were photographed, using a digital camera connected to a stereo-microscope (Nikon-SMZ 100, Japan). Then the wound area was measured by Image J software (ver 1.48, USA) [32]. Fish were identified individually by matching the pigmentation pattern of the caudal fin after taking a picture of the caudal fin. The wound area of individual fish was measured at the different time points. Each wounded area was identified based on the difference in skin color between wounded and unwounded areas. When the originally wounded area was no longer distinguishable (i.e., was completely regenerated and pigmented), each wound was considered as healed. The wound-healing effect of AgNPs was also quantified (as WHP) by examining the difference in wound size between 2 dpw and the other days (5, 7, 10 and 14 dpw) and expressing this as a percentage

187 relative to the 2 dpw wound size. A wound could only be visualized clearly by 2 dpw, therefore,
188 the first measurement was taken on that day.
189
190 2.6.2. *Histological analysis during wound healing*
191 To examine the effect of AgNPs on wound-healing activity in zebrafish, three fish at each
192 of 2, 5, 7, 10, 14, and 20 dpw were used from the histological experiment described in section
193 2.5. Fish were euthanized with an overdose of Tricaine (200 mg/L) by prolonged immersion and
194 fixed in 10% neutral buffered formalin for 24 h. The fish were then washed with running tap
195 water for 12 h. For decalcification, zebrafish were transferred to 0.5% EDTA (50 mL/fish) for 3
196 days and washed with running tap water for 12 h. Tissues were passed through a series of
197 increasing concentrations of ethanol (0–100%) in the tissue block of a Semi-enclosed Benchtop
198 Tissue Processor (Leica® TP1020, Germany) for dehydration in a slow and stepwise manner.
199 After dehydration, the tissue samples were embedded in paraffin (Leica® EG1150 Tissue
200 Embedding Center, Germany) and serial transverse sections (4 μm thick) (Leica® RM2125
201 microtome, Germany) were taken through the muscle tissues (control wound and AgNPs treated
202 wounds) and then stained with hematoxylin and eosin (H&E) (Sigma, Aldrich). The stained
203 tissue sections were observed under a light microscope (Leica® 3000 LED, Germany) and
204 images were captured by a digital camera (LEICA DCF450-C, Germany) connected to the
205 microscope.
206
207 2.7. *Quantitative real time polymerase chain reaction (qRT-PCR) analysis of inflammatory and*
208 *wound-healing genes*

For the gene expression analysis, zebrafish were divided into four groups of nine fish (n = 36). To the fish in the first group (under anesthesia) 2 µg of AgNPs were directly applied to the wound site on the day of wounding (0 dpw). Then fish were kept for 4 min outside, transferred to temporary recovery tank containing water for 5 min to get rid of excess AgNPs on the wound, and returned to the experimental tanks. The second group of wounded fish were immersed in an AgNPs-water (50 µg/L) solution, also kept outside for 4 min on 0 dpw with the AgNP-water solution changed on 0 dpw to simulate group 1 conditions. Similarly, for the third group, the wounded control fish were also kept outside for 4 min, and water changed to simulate group 1 and 2 conditions. An additional group was included as a control (no-wound group – negative control), and were also kept outside for 4 min, and water changed to simulate group 1, 2 and 3 conditions. From each of the four groups (negative control, wounded control, and two AgNPs-treated groups), muscle tissues from three zebrafish were collected at 12 hpw, 24 hpw and 5 dpw. Tissues were immediately snap frozen in liquid nitrogen and kept at −80 °C until RNA isolation using TRIzol® regent (Invitrogen, USA). From each experimental group, at each time point, muscle tissues from three fish were pooled (a total of 200 mg) for RNA isolation. Pooled RNA (2.5 µg) was used for cDNA synthesis using a PrimeScript 1st strand cDNA Synthesis Kit (TaKaRa®, Japan) according to the manufacturer's protocol. Using nuclease-free water, synthesized cDNA samples were diluted 30 times and stored at −20 °C until further use. For gene expression analysis, representatives of wound-healing-related genes, namely, transforming growth factor-β (TGF-β), matrix metalloproteinase (MMP) -9 and -13, pro-inflammatory cytokines (IL-1β and TNF-α) and antioxidant enzymes [superoxide dismutase (SOD) and catalase] were analyzed by qRT-PCR using a TaKaRa Thermal Cycler Dice TP 800 real-time system. The gene-specific primers are listed in Table 1. The qRT-PCR cycling protocol was

performed with a SYBR Premix Ex-Taq (Perfect Real Time) master mix (TaKaRa, Japan) in a total reaction volume of 10 µL containing 4 µL of cDNA, 5 µL of 2 × TaKaRa Ex-Taq™ SYBR premix and 0.5 µL of each forward and reverse primer (10 µM). The standard three-step thermal cycling profile of the machine with 55 °C annealing, followed by a single dissociation reading step at the end, was performed to identify the specificity of the primers. The relative expression "fold" was determined by the $2^{-\Delta\Delta CT}$ method described by Livak and Schmittgen [33]. Zebrafish β-actin was used as an internal reference gene to normalize the gene expression.

2.8. Statistical analysis

Statistical analysis of WHP data was performed by two-way analysis of variance (ANOVA) to find the overall significances between different experimental groups and time points, using GraphPad program ver. 6 (GraphPad Prism Software, Inc. USA). The means were then compared with both the Bonferroni post-test and an unpaired, two-tailed *t*-test. Significant differences were defined at $P < 0.05$. All data are represented as mean ± SD for triplicate reactions.

3. Results

3.1. Synthesis and physiochemical characterization of AgNPs

Appearance of an ash yellow color in the AgNPs aqueous solution (Fig. 2A) indicated the formation of AgNPs by chemical reduction of $AgNO_3$. This was confirmed by the presence of a maximum absorption peak around 390–400 nm, measured by UV visible spectroscopy [34]. The absorption at 400 nm (Fig. 2B) is a typical absorption band of spherical-shaped AgNPs due to their surface plasmon band [35]. Both FE-SEM and FE-TEM results indicated the circular shape

of the synthesized AgNPs (Fig. 2C, D). The average diameter of AgNPs was ~72.66 nm confirmed by particle size analysis (Fig. 2E), while a smaller particle size (~20 nm) was estimated by FE-TEM. The zeta-potential of AgNPs was −0.45 mv (Fig. 2F).

3.2. Effect of AgNPs toxicity in zebrafish

After zebrafish were exposed to different concentrations of AgNPs, the LD_{50} toxicity of AgNPs in zebrafish was determined as 140 µg/L. At the highest concentration (400 µg/L), AgNPs were highly toxic to exposed zebrafish and there was 100% mortality by 12 hpi (Fig. S1). In contrast, at 50 µg/L concentration, exposure to AgNPs resulted in no mortality and there was no toxicity behavior of fish up to 96 hpi.

3.3. Effect of AgNPs on wound healing

The wound-healing effect of AgNPs was determined by time-series visual observation of wound size (on 2, 5, 10 and 20 dpw) and WHP calculated on 5, 7, 10 and 14 dpw. Immediately after wounding (0 hpw), the laser-exposed area of the zebrafish showed as darker skin with or without mild hemorrhage, but the wound margins were not well enough defined to measure their areas. A wound with clear margins was first observed at 2 dpw and hence the first visual inspection of wound size was made on that day, with subsequent examinations on 5, 10 and 20 dpw (Fig. 3A). Both direct application and immersion treatments of AgNPs displayed obvious and faster wound closure at 5, 10 and 20 dpw compared to the control (Fig. 3A). At 20 dpw, no visible wound was observed in the AgNP-treated groups.

The wound-healing effect of AgNPs was quantified (expressed as WHP) at 5, 7, 10 and 14 dpw, relative to the wound size of day 2 (Fig. 3B). Wound size gradually decreased in all the

groups during 14-day healing period, showing an increase in WHP with time. The WHP was significantly higher ($P < 0.05$) in both AgNPs-treated groups (direct application and immersion) at all observations (Fig. 3B). Interestingly, immersion application of AgNPs was more efficient with a higher WHP than in the group subjected to AgNPs direct application. On day 5, WHP was 18.2%, 23.7% and 36.6% in the control, AgNPs direct application and AgNPs immersed groups, respectively. The comparable WHP values on 14 dpw were 68.3%, 74.8% and 78.8%, respectively.

3.4. Histology analysis during wound healing in zebrafish upon AgNPs treatment

Histological images, at two magnifications, of a transverse section through the laser-wounded tissues (skin and muscle) of untreated control zebrafish (Fig. 4A, D) were compared with images of the AgNPs direct application group (Fig. 4B, E) and AgNPs immersed group (Fig. 4C, F) at 5 dpw. H&E stained sectioning showed more recovered epidermis and dermis in the AgNPs-treated groups compared to the controls. In the untreated wounded tissues, the wound edge distance was longer (Fig. 4A, D) with a thin layer of epithelium (neo-epithelium). In AgNPs-treated fish the wound cavity was completely filled, whereas the wound cavity was deeper in the untreated fish (control group). It was apparent that epidermal cells had re-surfaced the wound in the AgNPs-treated fish, and a thick epithelium with densely packed dermal layer and well-forming granulation of tissues were evident, compared to the control. In the AgNPs immersion group in particular, epidermal cells had differentiated into well-formed skin and immune cells had aggregated near the wound margin. In addition, muscle cells in the AgNPs immersion group were already forming compared to the other groups, which had decomposed muscle cells in the wounded area.

301

302 *3.5. Transcriptional analysis of selected genes during wound healing upon AgNPs treatment*

303 Differential gene expression patterns in the fish muscles of the wounded control and two
304 AgNPs-treated groups were calculated comparative with gene expression in the negative (non-
305 wounded) control (Fig. 5).

306 3.5.1. TGF-β

307 Muscle TGF-β mRNA expression at 12 hpw was down regulated in the AgNPs-direct-
308 application group (0.5-fold) and the AgNPs immersion group (0.2-fold), more than in the
309 wounded control group, and all three expressions were lower than in the unwounded control
310 group (Fig. 5A). At 24 hpw, TGF-β was down regulated in the wounded control (0.5-fold) and
311 AgNPs direct applied group (0.7-fold), compared to the unwounded control whereas in the
312 AgNPs immersion group it was up regulated (1.6-fold). By 5 dpw, TGF-β expression in all
313 wounded groups had dropped below that of the negative control group.

314

315 3.5.2. IL-Iβ

316 IL-1β expression was highly up regulated in the wounded control group at 12 hpw (14.0-
317 fold) and 24 hpw (3.4-fold) (Fig. 5B). IL-1β expression in the AgNPs direct (10.5-fold) and
318 immersion (5.9-fold) treatment groups was higher at 12 hpw, but lower than in the wounded
319 group. At 24 hpw, IL-1β expression was higher in the wounded group (3.4-fold) and AgNPs
320 immersion group (3.2-fold) than in the negative control group, but it was close to base level in
321 the direct application group. At 5 dpw, gene expression levels were close to basal levels in all
322 groups although still slightly higher in both AgNPs-treated groups than in the control groups
323 (wounded and unwounded).

3.5.3. TNF-α

TNF-α expression in the muscle at 12 hpw showed down regulation (0.4–0.3-fold) in all the wounded groups (Fig. 5C). At 24 hpw, however, a higher up regulation of TNF-α was observed in the wounded (1.8-fold), direct AgNPs application (2.5-fold) and AgNPs immersion (2.0-fold) groups compared to the unwounded control. At 5 dpw, down regulation of TNF-α expression (0.04-fold) was observed in all three wounded groups compared to the negative control.

3.5.4. MMP-9

The expression pattern of MMP-9 in the zebrafish muscle was similar to that of IL1β and MMP-13. However, the magnitude of the expression was different at different time points (Fig. 5D). MMP-9 was markedly up regulated at 12 hpw in the wounded control (182.6-fold), AgNPs direct application (97.5-fold) and AgNPs immersion (73.7-fold) groups. At 24 hpw, there was a sharp drop in MMP-9 gene expression. Though it was high (3.7-fold) in the wounded control group, only slight induction (1.5–1.0-fold) was observed in the AgNPS-treated groups compared to the negative control. At 5 dpw, the gene expression pattern was similar to that observed at 12 hpw but the magnitude of expression was higher (between 3.0- and 4.8-fold) in the wounded groups compared to the negative control.

3.5.5. MMP-13

MMP-13 expression was up regulated in the wounded control (3.4-fold), AgNPs direct application (3.9-fold) and AgNP immersion (2.9-fold) groups compared to the negative control at

12 hpw (Fig. 5E). At 24 hpw, MMP-13 expression in the wounded control group was still up regulated (2.1-fold) although lower than at 12 hpw, and then the expression was down regulated (0.3-fold) at 5 dpw. At the same time (24 hpw), AgNPs-treated groups showed decreased (almost basal) mRNA expression compared to the wounded control group.

3.5.6. SOD

To investigate the potential involvement of reactive oxygen species (ROS) scavenging enzymes in the wound repair process, SOD and catalase mRNA expressions were analyzed (Fig. 5F, G). At 12 hpw, mRNA encoding SOD expression in the wounded control tissue was slightly lower (0.8-fold) than in the tissues of the negative control. However, it was up regulated (2.1-fold) at 24 hpw. Subsequently, at 5 dpw expression declined (0.2-fold) compared with the non-wounded control. In contrast, up regulation of SOD mRNA levels was observed at 12 hpw in both the AgNPs direct application (1.2-fold) and AgNPs immersion (2.0-fold) groups. SOD expression at 24 hpw in the AgNPs direct application group was higher (1.65-fold) than in the negative control and down regulated (0.3-fold) at 5 dpw. In the AgNPs immersion group, the SOD expression levels were similar to the negative control at 24 hpw and 5 dpw.

3.5.7. Catalase

At 12 hpw, the catalase mRNA expression pattern was mostly similar to the SOD expression pattern with slight variation in the direct AgNPs application group (Fig. 5G). At 24 hpw, both in the wounded control (2.0-fold) and AgNPs direct application (6.3-fold) groups, up regulation was observed. However, expression in the AgNPs immersion group was basal level at

24 dpw. At 5 dpw, the expression patterns of catalase mRNA were similar to the SOD mRNA expression at the same time point.

4. Discussion

Knowing the particle size, surface area and zeta potential is essential to gain mechanistic information of NPs uptake, persistence and biological toxicity within cells [36]. Hence, designing a simple AgNPs synthesis method that gives consistent size, morphology, stability and properties is essential to obtain consistent results when AgNPs were applied to biological systems at relatively non-toxic concentrations [37].

In this study, zebrafish were used to investigate the AgNPs effect on wound-healing activity in zebrafish after laser-induced wound injury. Firstly, we determined the toxic effect of the synthesized AgNPs in a zebrafish model. The LD_{50} of the synthesized AgNPs was found to be 140 µg/L and zebrafish exposed to 50 µg/L did not show any toxicity signs. Bilberg et al. [38] reported that the LC_{50} of AgNPs (average size 81 nm) in zebrafish is 84 µg/L at 48 hpi, and that at >72 µg/L AgNPs, signs of toxicity stress emerged. Secondly, two treatment methods were applied in our study and both AgNPs direct application and AgNPs immersion displayed clear and faster wound healing at 5, 10 and 20 dpw compared to the wounded controls. Interestingly, AgNPs application by immersion had a higher WHP than AgNPs applied directly, showing that AgNPs immersion induced a faster healing rate. Mathivanan et al. [30] reported that a 20% AgNPs solution has an impact on wound healing in the fresh water fish *Anaba testudineus.* AgNPs release a cluster of uncharged Ag atoms (Ag^0) and Ag^+. Those uncharged Ag reacts slowly with chloride in the wound exudate which increases the efficacy of the wound healing action [39, 40]. Similarly, we suggest our AgNPs with Ag atoms may slower the reaction with

chloride at the wound site and thereby enhance the wound healing process. Our data indicate that immersion in AgNPs solution could be useful for treating ornamental fish because it is much more convenient than treating individual fish by AgNPs direct treatment. Moreover, from our visual and quantified wound healing data, we confirm that the AgNPs synthesized in this study and their physiochemical properties were ideal to exert wound-healing activity without showing toxicity to the zebrafish.

Most of the steps and principles of wound healing are conserved in adult mammals and zebrafish [41]. The major difference between mammalian and zebrafish wound repair is that in fish, remodeling of wound tissue occurs with minimum scarring. Even when deeper wound damage was present, including of muscles, skin regenerated almost completely and more quickly; however, the damaged muscle did not [41]. Based on our histology data, it was difficult to observe in detail all the wound-healing processes described by others [41]. However, recovering epidermis, dermis and muscle were observed at different magnitudes in the wounds of AgNPs-treated groups compared with the control groups at 5 dpw (Fig. 4) and 7 dpw (data not shown). At the last stage of the healing process (20 dpw), the skin of zebrafish of both AgNPs treatment groups appeared completely normal, with minimal scarring compared to wounded untreated fish. The tissue-regenerating capacity of organisms differs and the time course of each individual wound-healing process varies by fish species [30, 42, 43]. Moreover, it is dependent on the age and physiological condition of the fish, the extent of damage, cause of wounding, the depth of tissue and nutritional status of the individual [41,44]. Detailed immunofluorescence or immune-histochemistry studies are required to study each of the healing processes in a systematic manner, in addition to histopathology.

Immune inflammatory cells (lymphocytes, monocytes and neutrophils) are the main cellular immune components that control inflammatory reactions and the subsequent repair process [43, 45]. These cells play a major role in initiating inflammation, and also in the progression and regulation of the repair process. For a deeper understanding of the AgNPs' effect on wound healing in zebrafish, the transcriptional responses of genes representative of early phases of wound healing were studied, especially focusing on the inflammatory response genes. Among the earliest signal initiation molecules, the growth factor TGF-β, which is released during hemostasis, is important in wound healing [6, 14, 46]. It has been described that the various growth factors released during homostasis to regulate the stimulation and recruitment of monocytes, neutrophils and macrophages to the wound site, thereby initiating the inflammatory phase [46]. However, the magnitude and duration of inflammatory responses are factors that play a major role in the wound-healing process and it is important to limit the inflammatory process to avoid chronic scarring [2].

Matrix metalloproteinases (MMPs) are involved in all phases of wound healing by modulating the influx of immune cells, enhancing fibroblasts and keratinocytes migration and scar tissue remodeling. During the inflammatory phase, macrophages secrete MMPs to remove debris from the wound site to enhance the healing process [46]. Generally the pro-inflammatory cytokines, IL-1 and TNF-α, at inflammatory sites result in the stimulation of MMP gene expression [47]. There is credible evidence for increased MMPs expression, including of MMP-9 (gelatinases) and MMP-13 (collagenases), during wound repair at different phases of wound healing, including epithelial migration, angiogenesis, granulation, tissue formation and wound contraction [41, 48–51].

436 In Japanese flounder, Murakami et al. [52] suggested that MMP-9 may be essential
437 during wound healing for re-epithelization and the process of inflammatory cell migration, as
438 many inflammatory cells were detected in the dermis at 24 hpw. In vertebrates, MMP-13 is
439 known to catalyze the degradation of type I collagens at neutral pH. In zebrafish, MMP-13
440 expression has been shown in normal embryonic development [53]. Previous studies showed
441 marked up regulation of IL-1β, MMP-9, MMP-13 and TGF-β in the muscles of experimentally
442 wounded rainbow trout at early post-wounding time points (1–14 dpw) and a sharp reduction
443 thereafter. However, the transcription remained higher than in the external controls [43].
444 Additionally, in the muscle of wounded carp, IL-1β, IL-6 and IL-8 at 1 dpw were all up regulated
445 but declined later [54]. In the current study, wound-healing genes differentially responded based
446 on the treatment and time of measurement. Mostly, zebrafish treated by direct application of
447 AgNPs showed a higher expression than the AgNPs-immersed animals, but mostly lower than in
448 the wounded controls. It has been reported that, if the activities of the MMPs are not properly
449 controlled, wound healing could be impaired and reach chronic stage [55–57]. The MMP-9 and
450 MMP-13 expression patterns at 12 hpw and 5 dpw in our study suggest that no adverse effects on
451 wound healing were caused by the AgNPs treatment and that the normal wound-healing process
452 had taken place.

453 The importance of ROS generation in wound healing is well documented for
454 inflammation, cell migration, proliferation and angiogenesis [58–61]. To investigate the potential
455 involvement of ROS scavenging enzymes in the wound-healing process, SOD and catalase
456 mRNA expression were analyzed, because these have not so far been reported in detail in
457 zebrafish. Since O_2^- is the major ROS generated during the respiratory burst of inflammatory
458 cells [62, 63], we first analyzed SOD expression in the unwounded negative control, wounded

control and AgNPs-treated groups. Though the SOD was slightly down regulated at 12 hpw in the wounded fish, it was up regulated at 24 hpw. There was slight up regulation of SOD mRNA expression following AgNPs direct application, and then it was further increased at 24 hpw. Marked 2-fold up regulation was observed in the AgNPs immersed group at 12 hpw, but it returned to basal levels at 24 hpw and 5 dpw. At 5 dpw, a down regulated SOD expression pattern was observed in wounded and AgNPs-direct-application zebrafish. At this level, it is difficult to discuss logically the exact reason for the differential expression pattern (down regulation at wounded tissue), whether the down regulation occurred due to the physiological condition of the animal or another factor (e.g. stress or due to alteration of regulatory mechanisms).

It has been reported that the cytosolic Cu/Zn-dependent SOD (SOD1) and mitochondrial Mn-dependent SOD (SOD2) mRNA levels were up regulated in the healing wounds of mice skin and that the highest expression was observed in the early inflammatory phase. Similarly, in SOD1-knockout-wounded mice the wound-healing time is delayed [64]. Similar patterns of both catalase and SOD mRNA expressions were observed in this study. The biological mechanism of the co-expression pattern of SOD and catalase to counteract ROS species is very important [65]. Taken together, these results demonstrate that the mRNA expression of both SOD and catalase is elevated at certain times during the wound repair process. The increased expression of these molecules after injury suggests that SODs and peroxidases/catalase play an important role in the detoxification of ROS in wounded environments. Our data indicate that a higher level of ROS might have been generated during the inflammation process in the AgNPs immersion group compared to the other groups and thereafter, the redox balance is established at the correct time, thus promoting efficient wound healing. This is consistent with our visual observations, and

482 further confirms rapid wound healing in zebrafish exposed to AgNPs especially in the ones
483 immersed in AgNPs.

484 In summary, chemically synthesized AgNPs had a better effect on wound-healing activity
485 compared to the normal wound-healing process in our zebrafish model. Fish immersion in an
486 AgNPs-water solution (50 µg/L) resulted in a speedier healing time compared with direct
487 application of AgNPs to the wounded area. AgNPs, either applied directly to wounded skin or
488 wounded animals immersed in AgNPs solution, showed differential gene expression patterns in
489 the inflammatory, proteases, growth factor and antioxidant genes studied, indicating varying
490 transcription effects for efficient wound healing. Collectively, from the gene expression data, and
491 evidence from previously published wound healing information [30, 41, 46], we could postulate
492 that AgNPs as a wound treatment did not affect the co-ordinated migration of the different cell
493 types and signaling events, and maintained the molecular functions and redox balance to avoid
494 sustained inflammation, to promote efficient wound-healing processes without causing scarring.
495 A clear understanding of the different molecules' functions and mechanisms in the process of
496 wound healing and their temporal expression pattern on exposure to AgNPs in zebrafish and/or
497 other vertebrates is needed. Further studies will be conducted to elucidate the role of AgNPs as a
498 wound-healing agent in fish since it appears to be a promising candidate for use in wound care
499 therapy.

500

501 **Acknowledgements**

502 This work was supported by a National Research Foundation of Korea (NRF) grant funded by
503 the Korean government (MSIP) (2014R1A2A1A11054585).

504

505 **References**

506 [1] Fantone JC, Ward PA. Role of oxygen-derived free radicals and metabolites in leukocyte-
507 dependent inflammatory reactions. Am J Pathol 1982;107:395–418.
508 [2] Kovacs EJ, Dipietro LA. Fibrogenic cytokines and connective-tissue production. Faseb J
509 1994;8:854–61.
510 [3] Julliard AK, Saucier D, Astic L. Time-course of apoptosis in the olfactory epithelium of
511 rainbow trout exposed to a low copper level. Tissue Cell 1996;28:367–77.
512 http://dx.doi.org/10.1016/S0040-8166(96)80023-1
513 [4] Noga EJ. Skin ulcers in fish: Pfiesteria and other etiologies. Toxicol Pathol 2000;28:807–23.
514 [5] Ellis T, North B, Scott AP, Bromage NR, Porter M, Gadd D. The relationships between
515 stocking density and welfare in farmed rainbow trout. J Fish Biol 2002;61:493–531.
516 http://dx.doi.org/10.1111/j.1095-8649.2002.tb00893.x
517 [6] Ashley PJ. Fish welfare: Current issues in aquaculture. Appl Anim Behav Sci 2007;104:199–
518 235. http://dx.doi.org/10.1016/j.applanim.2006.09.001
519 [7] Frommel AY, Maneja R, Lowe D, Malzahn AM, Geffen AJ, Folkvord A, Piatkowski U,
520 Reusch TBH, Clemmesen C. Severe tissue damage in Atlantic cod larvae under increasing
521 ocean acidification. Nature Clim Change 2011;2:42–6.
522 http://dx.doi.org/10.1038/nclimate1324
523 [8] Lushchak VI. Environmentally induced oxidative stress in aquatic animals. Aquat Toxicol
524 2011;101:13–30. http://dx.doi.org/10.1016/j.aquatox.2010.10.006
525 [9] Jeney Z, Jeney G. Recent achievements in studies on diseases of common carp (*Cyprinus-*
526 *carpio* L.). Aquaculture 1995:129:397–420. http://dx.doi.org/10.1016/0044-8486(94)00283-
527 T
528 [10] Johnson SC, Treasurer JW, Bravo S, Nagasawa K, Kabata Z. A review of the impact of
529 parasitic copepods on marine aquaculture. Zool Stud 2004;43:229–43.
530 [11] Ingerslev HC, Lunder T, Nielsen ME. Inflammatory and regenerative responses in
531 salmonids following mechanical tissue damage and natural infection. Fish Shellfish Immun
532 2010;29:440–50. http://dx.doi.org/10.1016/j.fsi.2010.05.002
533 [12] Martin P. Wound healing – Aiming for perfect skin regeneration. Science 1997;276:75–81.
534 http://dx.doi.org/10.1126/science.276.5309.75

[13] Singer AJ, Clark RAF. Cutaneous wound healing. N Engl J Med 1999;341:738–46.

[14] Gurtner GC, Werner S, Barrandon Y, Longaker MT. Wound repair and regeneration. Nature 2008;453:314–21. http://dx.doi.org/10.1038/nature07039

[15] Koh TJ, DiPietro LA. Inflammation and wound healing: The role of the macrophage. Expert Rev Mol Med 2013;13:e23. http://dx.doi.org/10.1017/S1462399411001943

[16] Valluru M, Staton CA, Reed MWR, Brown NJ. Transforming growth factor-beta and endoglin signaling orchestrate wound healing. Front Physiol 2011;2:1–12.

[17] Sabino F, Keller UAD. Matrix metalloproteinases in impaired wound healing. Metalloproteinases Med 2015;2:1–8.

[18] Saettone MF, Salminen L. Ocular inserts for topical delivery. Adv Drug Deliv Rev 1995;16:95–106. http://dx.doi.org/10.1016/0169-409X (95)00014-X

[19] Singh R, Lillard JW Jr. Nanoparticle-based targeted drug delivery. Exp Mol Pathol 2009;86:215–23. http://dx.doi.org/10.1016/j.yexmp.2008.12.004

[20] Can E, Kizak V, Kayim M, Can SS, Kutlu B, Ates M, Kocabas M, Demirtas N. Nanotechnological applications in aquaculture-seafood industries and adverse effects of nanoparticles on environment. J Mater Sci Eng 2011;5:605–9.

[21] Vazquez JA, Rodríguez-Amado I, Montemayor MI, Fraguas J, Gonzalez MP, Murado MA. Chondroitin sulfate, hyaluronic acid and chitin/chitosan production using marine waste sources: characteristics, applications and eco-friendly processes: A review. Mar Drugs 2013;11:747–74.

[22] http://www.nanotechproject.org/process/assets/files/7039/silver_database_fauss_sept2_final.pdf

[23] Soltani M, Ghodratnema M, Ahari H, Ebrahimzadeh Mousavi HA, Atee M, Dastmalchi F, Rahmanya J. The inhibitory effect of silver nanoparticles on the bacterial fish pathogens, *Streptococcus iniae*, *Lactococcus garvieae*, *Yersinia ruckeri* and *Aeromonas hydrophila*. Int J Vet Res 2009;3:137–142.

[24] Wright JB, Lam K, Hansen D, Burrell RE. Efficacy of tropical silver against fungal burn wound pathogens. Am J Inf Cont 1999;27:344–50.

[25] Fong J, Wood F. Nanocrystalline silver dressings in wound management: a review. Int J Nanomed 2006;1:441–9. http://dx.doi.org/10.2147/nano.2006.1.4.441

566 [26] Demling RH, DeSanti L. The role of silver technology in wound healing: Part 1: Effects of
567 silver on wound management. Wounds 2001;13(Suppl A):4–15.
568 [27] Lee DY, Fortin C, Campbell PGC. Contrasting effects of chloride on the toxicity of silver to
569 two green algae, *Pseudokirchneriella subcapitata* and *Chlamydomonas reinhardtii*. Aquat
570 Toxicol 2005;75:127–35. http://dx.doi.org/10.1016/j.aquatox.2005.06.011
571 [28] Tappin AD, Barriada JL, Braungardt CB, Evans EH, Patey MD, Achterberg EP. Dissolved
572 silver in European estuarine and coastal waters. Water Res 2010;44:4204–16.
573 http://dx.doi.org/10.1016/j.watres.2010.05.022
574 [29] Eom HJ, Choi J. p38 MAPK activation, DNA damage, cell cycle arrest and apoptosis as
575 mechanisms of toxicity of silver nanoparticles in Jurkat T cells. Environ Sci Technol
576 2010;44:8337–42. http://dx.doi.org/10.1021/es1020668
577 [30] Mathivanan V, Ananth S, Priyanga B, Ganesh Prabu P, Selvisabhanayakam. Impact of
578 silver nanoparticles on wound healing of freshwater fish, *Anabas testudineus*. Int J Res Fish
579 Aqua 2012;2:17–21.
580 [31] Xu H, Suslick KS. Water-soluble fluorescent silver nanoclusters. Adv Mater 2010;22:1078–
581 82. http://dx.doi.org/10.1002/adma.200904199
582 [32] Abramoff MD, Magalhães PJ, Ram SJ. Image processing with Image J. Biophotonics Int
583 2004;11:36–42.
584 [33] Livak KJ, Schmittgen TD. Analysis of relative gene expression data using real-time
585 quantitative PCR and the $2^{-\Delta\Delta C}$T. Methods 2001;25:402–8.
586 [34] Huang H, Yang X. Synthesis of polysaccharide-stabilized gold and silver nanoparticles: a
587 green method. Carbohydrate Res 2004;339:2627–31.
588 http://dx.doi.org/10.1016/j.carres.2004.08.005
589 [35] Kim JS, Kuk E, Yu KN, Kim JH, Park SJ, Lee HJ, Kim SH, et al. Antimicrobial effects of
590 silver nanoparticles. Nanomed Nanotech Biol Med 2007;3:95–101.
591 http://dx.doi.org/10.1016/j.nano.2006.12.001
592 [36] Karakoti AS, Hench LL, Seal S. The potential toxicity of nanomaterials – The role of
593 surfaces. JOM 2006;58:77–82. http://dx.doi.org/10.1007/s11837-006-0147-0
594 [37] Wiley B, Sun Y, Xia Y. Synthesis of silver nanostructures with controlled shapes and
595 properties. Acc Chem Res 2007;40:1067–76. http://dx.doi.org/10.1021/ar7000974

596 [38] Bilberg K, Hovgaard MB, Besenbacher F, Baatrup E. *In vivo* toxicity of silver nanoparticles
597 and silver ions in zebrafish (*Danio rerio*). J Toxic 2012;1–9.
598 http://dx.doi.org/10.1155/2012/293784
599 [39] Widgerow AD. Nanocrystalline silver, gelatinases and the clinical implications. Burns
600 2010;36:965–74. http://dx.doi.org/10.1016/j.burns.2010.01.010
601 [40] Politano AD, Campbell KT, Rosenberger LH, Sawyer RG. Use of silver in the prevention
602 and treatment of infections: silver review. Surg Infect 2013;14:8–20.
603 http://dx.doi.org/10.1089/sur.2011.097
604 [41] Richardson R, Slanchev K, Kraus C, Knyphausen P, Eming S, Hammerschmidt M. Adult
605 zebrafish as a model system for cutaneous wound-healing research. J Invest Dermatol
606 2013;133:1655–65. http://dx.doi.org/10.1038/jid.2013.16
607 [42] Dutta M, Rai AK. Pattern of cutaneous wound healing in a live fish *Clarias batrachus* (L.)
608 (Clariidea, Pisces.). J Indian Fish Assoc 1994;24:107–13.
609 [43] Schmidt JG, Andersen EW, Ersboll BK, Nielsen ME. Muscle wound healing in rainbow
610 trout (*Oncorhynchus mykiss*). Fish Shellfish Immun 2016;48:273–84.
611 http://dx.doi.org/10.1016/j.fsi.2015.12.010
612 [44] Enoch S, Harding KG. Wound bed preparation: The science behind the removal of barriers
613 to healing. Wounds 2003;15:213–29.
614 [45] Agaiby AD, Dyson M. Immuno-inflammatory cell dynamics during cutaneous wound
615 Healing. J Anat 1999;195,531–42.
616 [46] Valluru M, Staton CA, Reed MWR, Brown NJ. Transforming growth factor-β and endoglin
617 signaling orchestrate wound healing. Front Physiol 2011;2:1–12.
618 [47] Chakraborti S, Mandal M, Das S, Mandal A, Chakraborti T. Regulation of matrix
619 metalloproteases: An overview. Mol Cell Biochem 2003;253:269–85.
620 [48] Stadelmann WK, Digenis AG, Tobin GR. Physiology and healing dynamics of chronic
621 cutaneous wounds. Am J Surg 1998;176(2A Suppl):26S–38S.
622 http://dx.doi.org/10.1016/S0002-9610 (98)00183-4
623 [49] O'Toole EA. Extracellular matrix and keratinocyte migration. Clin Exp Dermatol
624 2001;26:525–30. http://dx.doi.org/10.1046/j.1365-2230.2001.00891.x

[50] Parks WC, Wilson CL, Lopez-Boado YS. Matrix metalloproteinases as modulators of inflammation and innate immunity. Nat Rev Immunol 2004;4:617–29. http://dx.doi.org/10.1038/nri1418

[51] Chen P, Parks WC. Role of matrix metalloproteinases in epithelial migration. J Cell Biochem 2009;108:1233–43. http://dx.doi.org/10.1002/jcb.22363

[52] Murakami A, Mano N, Rahman MH, Hirose H. MMP-9 is expressed during wound healing in Japanese flounder skin. Fisheries Sci 2006;72:1004–10. http://dx.doi.org/10.1111/j.1444-2906.2006.01249.x

[53] Hillegass JM, Villano CM, Cooper KR, White LA. Matrix metalloproteinase-13 is required for zebra fish (*Danio rerio*) development and is a target for glucocorticoids. Toxicol Sci 2007;100:168–79. http://dx.doi.org/10.1093/toxsci/kfm192

[54] Przybylska-Diaz DA, Schmidt JG, Vera-Jimenez NI, Steinhagen D, Nielsen ME. Beta-glucan enriched bath directly stimulates the wound healing process in common carp (*Cyprinus carpio* L.). Fish Shellfish Immun 2013;35:998–1006.

[55] Menke MN, Menke NB, Boardman CH, Diegelmann RF. Biologic therapeutics and molecular profiling to optimize wound healing. Gynecol Oncol 2008;111(2 Suppl):S87–91. http://dx.doi.org/10.1016/j.ygyno.2008.07.052

[56] Widgerow AD. Chronic wound fluid – thinking outside the box. Wound Repair Regen 2011;19:287–91. http://dx.doi.org/10.1111/j.1524-475X.2011.00683.x

[57] Martins VL, Caley M, O'Toole EA. Matrix metalloproteinases and epidermal wound repair. Cell Tissue Res 2013;351:255–68. http://dx.doi.org/10.1007/s00441-012-1410-z

[58] Vivekananda J, Lin A, Coalson JJ, King RJ. Acute Inflammatory injury in the lung precipitated by oxidant stress induces fibroblasts to synthesize and release transforming growth-factor-alpha. J Biol Chem 1994;269:25057–61.

[59] Niethammer P, Grabher C, Look AT, Mitchison TJ. A tissue-scale gradient of hydrogen peroxide mediates rapid wound detection in zebrafish. Nature 2009;459:996–9. http://dx.doi.org/10.1038/nature08119

[60] Kanta J. The role of hydrogen peroxide and other reactive oxygen species in wound healing. Acta Medica (Hradec Kralove) 2011;54:97–101. http://dx.doi.org/10.14712/18059694.2016.28

[61] Breton-Romero R, Lamas S. Hydrogen peroxide signaling in vascular endothelial cells. Redox Biol 2014;2:529–34. http://dx.doi.org/10.1016/j.redox.2014.02.005

[62] Goldman R. Growth factors and chronic wound healing; Past, present, and future. Adv Skin Wound Care 2004;17:24–35. http://dx.doi.org/10.1097/00129334-200401000-00012

[63] Martin P, Leibovich SJ. Inflammatory cells during wound, repair: the good, the bad and the ugly. Trends Cell Biol 2005;15:599–607. http://dx.doi.org/10.1016/j.tcb.2005.09.002

[64] Iuchi Y, Roy D, Okada F, Kibe N, Tsunoda S, Suzuki S, Takahashi M et al. Spontaneous skin damage and delayed wound healing in SOD1-deficient mice. Mol Cell Biochem 2010;341:181–94. http://dx.doi.org/10.1007/s11010-010-0449-y

[65] Steiling H, Munz B, Werner S, Brauchle M. Different types of ROS-scavenging enzymes are expressed during cutaneous wound repair. Exp Cell Res 1999;247:484–94. http://dx.doi.org/10.1006/excr.1998.4366

668 **Table 1**
669 Primer information of the zebrafish genes selected for this study.

Gene name	Accession number	Primer name	Primer sequence (5'-3')
Transforming growth factor-β (TGF-β)	XM_687246	TGF-β-F	CCCAAGGAACCAGAAGTAGAAG
		TGF-β-R	GGATCTTCTATGGTGTGCTGAA
Interleukin 1β (IL-1β)	AY340959.1	IL-1β-F	TCAAACCCCAATCCACAGAG
		IL-1β-R	TCACTTCACGCTCTTGGATG
Tumor necrosis factor-α (TNF-α)	AY427649	TNF-α-F	AGAAGGAGAGTTGCCTTTACCGCT
		TNF-α-R	AACACCCTCCATACACCCGACTTT
Matrix metalloproteinase (MMP) -9	AY151254	MMP-9-F	TTTGCCCTGATCGTGGATAC
		MMP-9-R	GGGAAACCCTCCACGTATTT
Matrix metalloproteinase (MMP) -13	AF506756	MMP-13-F	GAGAAGGTTTGGGCTCTCTATG
		MMP-13-R	TGAGTTGCTGTCTTCCTTGTAG
Superoxide dismutase (SOD)	NM_131294.1	SOD-F	AGGTGACTGGTGAAATTACTGG
		SOD-R	GTCTCACACTATCGGTTGGC
Catalase	NM_130912.2	Catalase-F	CCAAGGTCTGGTCCCATAAAG
		Catalase-R	GCTCAACCTCCGCGAAATA
β-actin	AF025305	β-actin-F	AATCTTGCGGTATCCACGAGACCA
		β-actin-R	TCTCCTTCTGCATCCTGTCAGCAA

670

671 **Figure legends**

672 **Fig. 1.** Position of the laser wound created on the zebrafish (in red circle). On the anesthetized
673 fish, a laser wound was created with a laser beam (150 mA for 5 s), posterior to the gill area,
674 close to the lateral line of the zebrafish.
675
676 **Fig. 2.** Physiochemical characterization of AgNPs. (A) Newly synthesized water-soluble AgNPs,
677 (B) UV-vis spectrum, (C) FE-SEM image, (D) FE-TEM image, (E) particle size distribution
678 (72.66 nm) and (F) zeta-potential (-0.45 mV) of AgNPs.
679
680 **Fig. 3.** Wound-healing effects of AgNPs on adult zebrafish. (A) Representative pictures of
681 wound-healing process of zebrafish at 2, 5, 10 and 20 dpw. Images exhibit significantly reduced
682 wound size on zebrafish in AgNPs-treated groups comparative to the control groups at 5 and 10
683 dpw. (B) WHP at 5, 7, 10 and 14 dpw on the zebrafish. On each day WHP was calculated based
684 on the wound size at 2 dpw. Bars represent the mean $\pm$ SD (n = 12).
685
686 **Fig. 4.** H&E stained histology images showing transverse sections through the laser-damaged
687 wounded tissue (including skin and muscle) of zebrafish at 5 dpw: (A and D) Control-untreated,
688 (B and E) AgNPs direct application and (C and F) AgNPs water immersion treated. A, B and C:
689 200×; D, E and F: 400×. Wounded area marked in dotted square. EP: epithelium, SC: scales, SP:
690 scale pockets, WE: wounded edge, WC: wound cavity, SM: skeletal muscle. Thin black arrow:
691 thin epithelium with immune cell infiltration; thick black arrow: formation of epithelium layer;
692 red arrows: disintegrated muscle cells in dermal layer. White arrows: densely packed muscle
693 cells.
694
695 **Fig. 5.** Relative mRNA expression of wound-healing-related genes of adult zebrafish muscle at
696 12 hpw, 24 hpw and 5 dpw after AgNPs direct application (grey) and AgNPs immersion
697 treatments (blue) compared with the wounded controls (orange) and non-wounded negative
698 controls (green). (A) TGF-β, (B) IL-1β, (C) TNF-α, (D) MMP-9, (E) MMP-13, (F) SOD and (G)
699 Catalase. Relative expression folds of each gene were calculated according to the Livak method
700 ($2^{-\Delta\Delta CT}$) [33]. Zebrafish β-actin was used as a house-keeping gene. Fold units were calculated
701 dividing the normalized expression values of the treatment by that of the respective control at
702 each time point. Data represent the mean of three independent qPCR reactions for technical
703 reproducibility using the cDNA, which corresponds to the pooled RNA of three fish, and bars
704 represent the mean $\pm$ SD of three independent qPCR reactions.
705

706 **Figures**

707

708

709

710 Fig. 1.

711

712

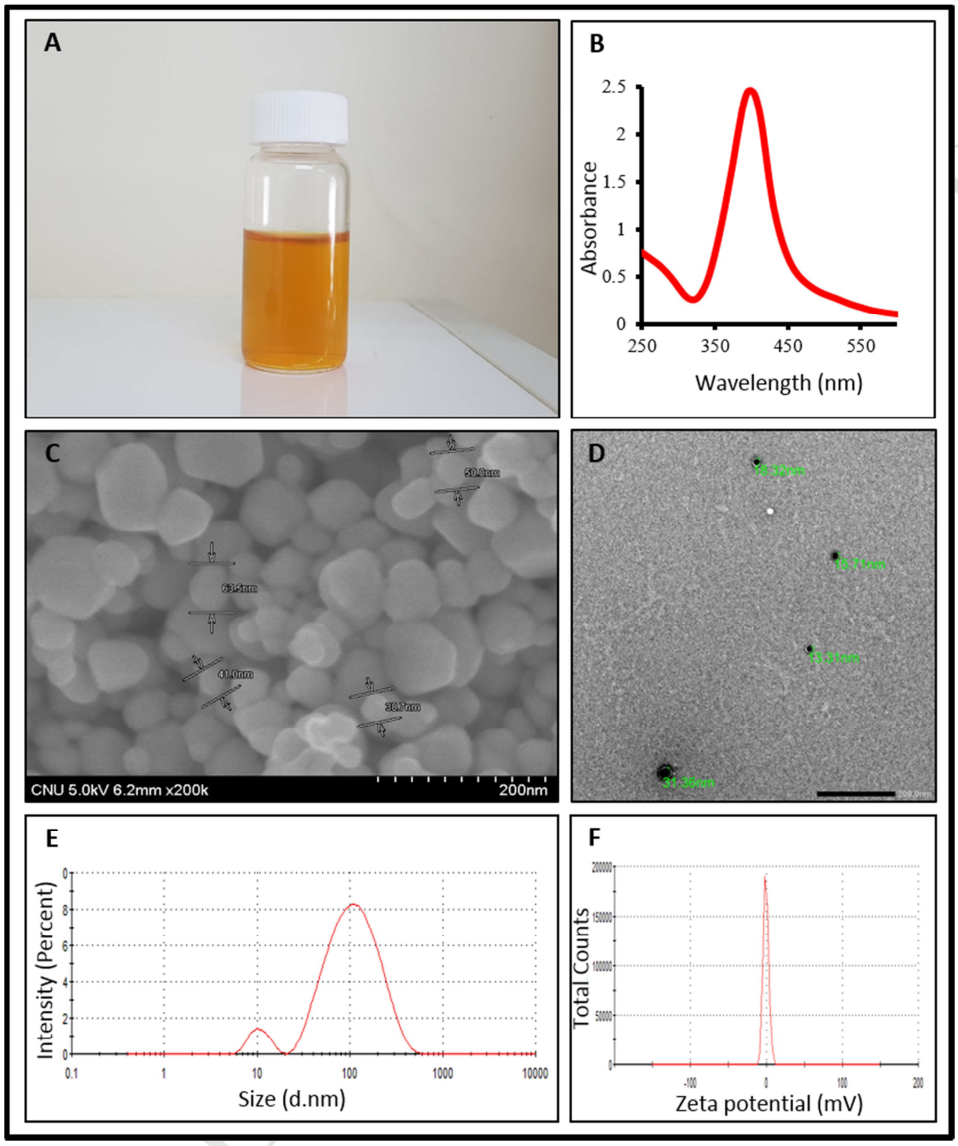

713

714

715 Fig. 2.

716

717

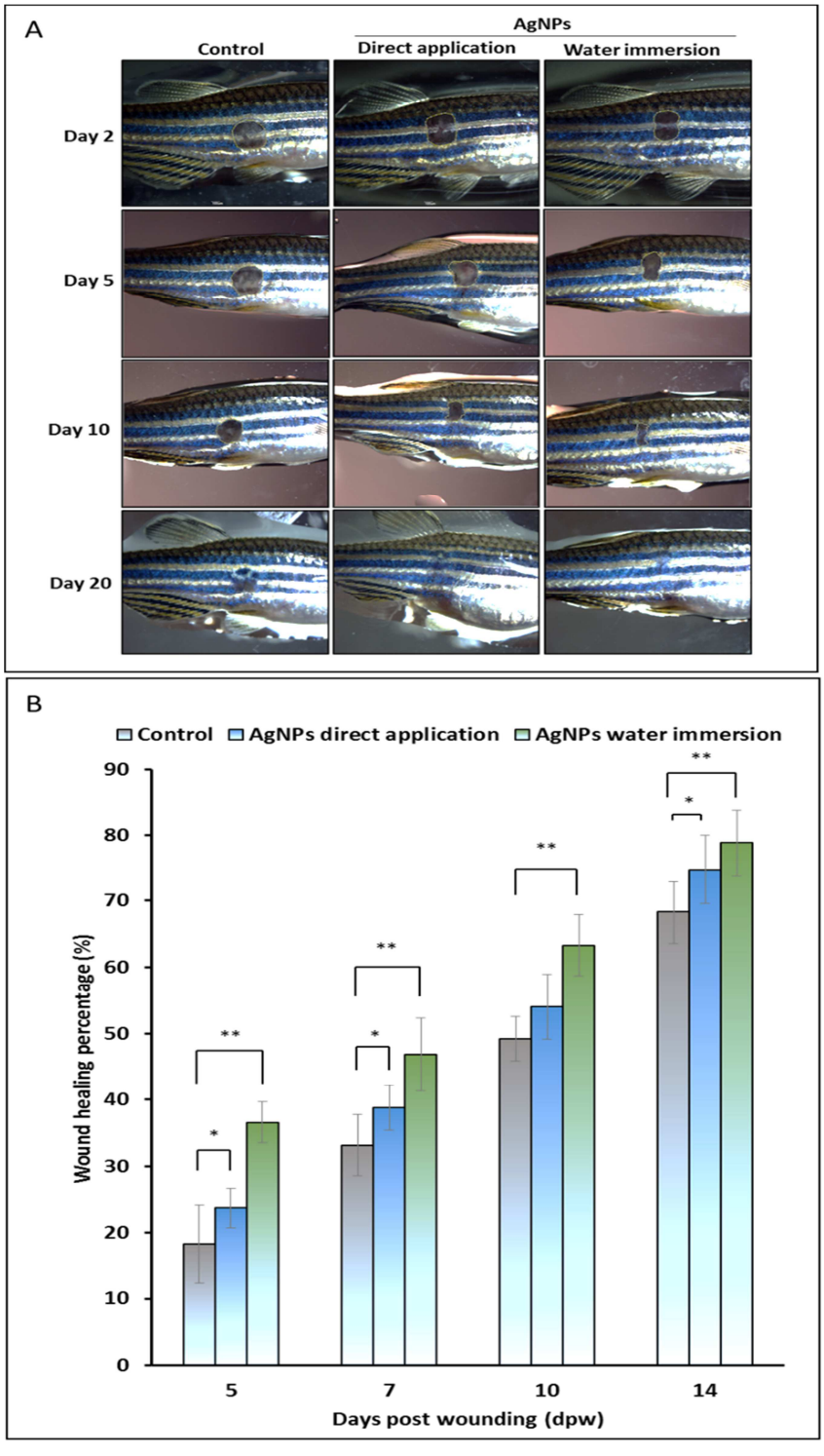

718

719 Fig. 3.

720

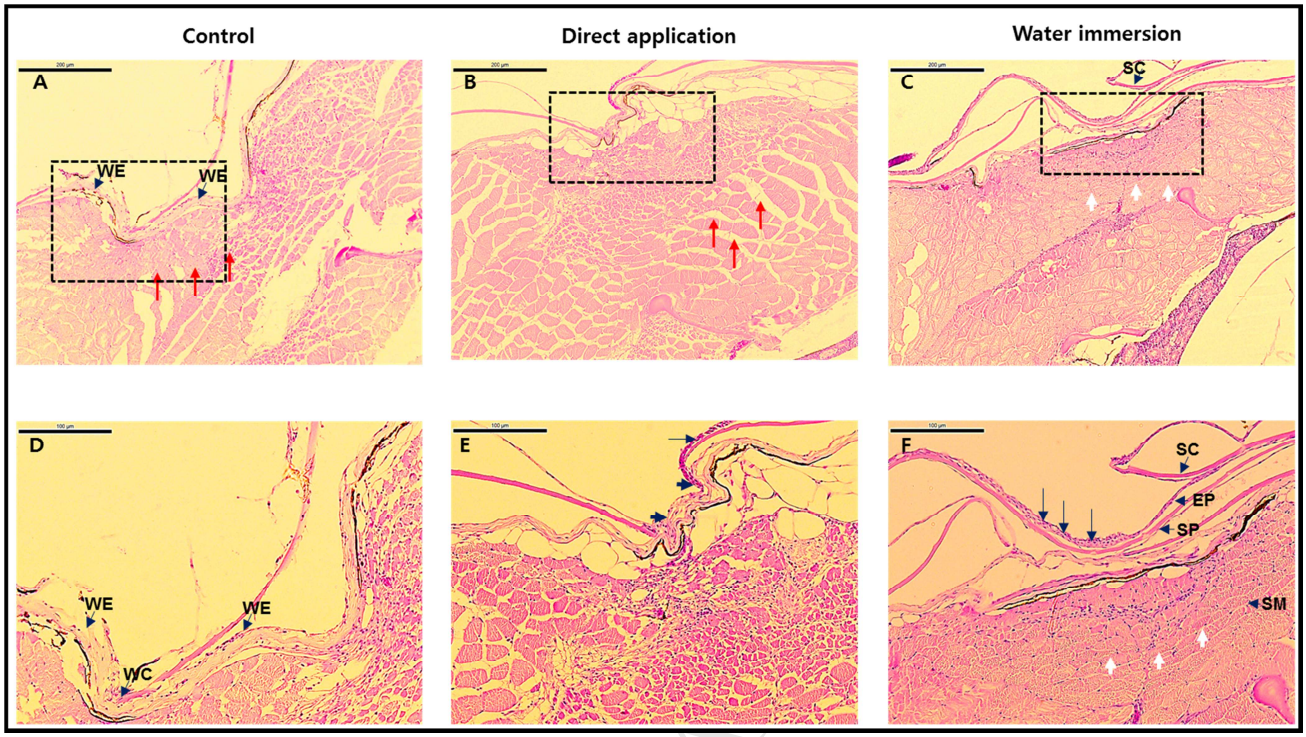

Fig. 4.

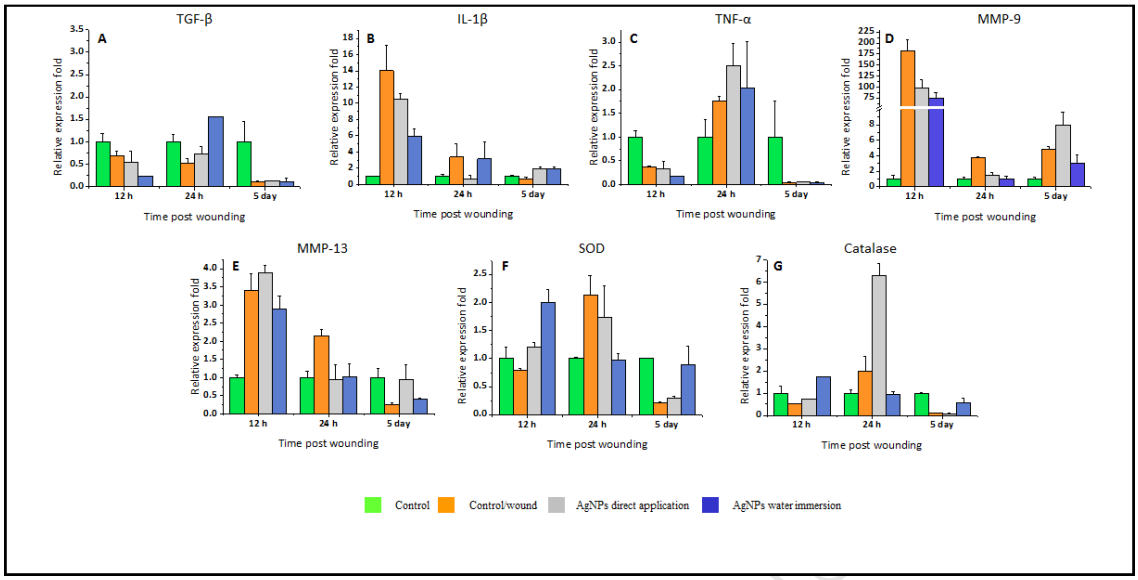

Fig. 5.

730

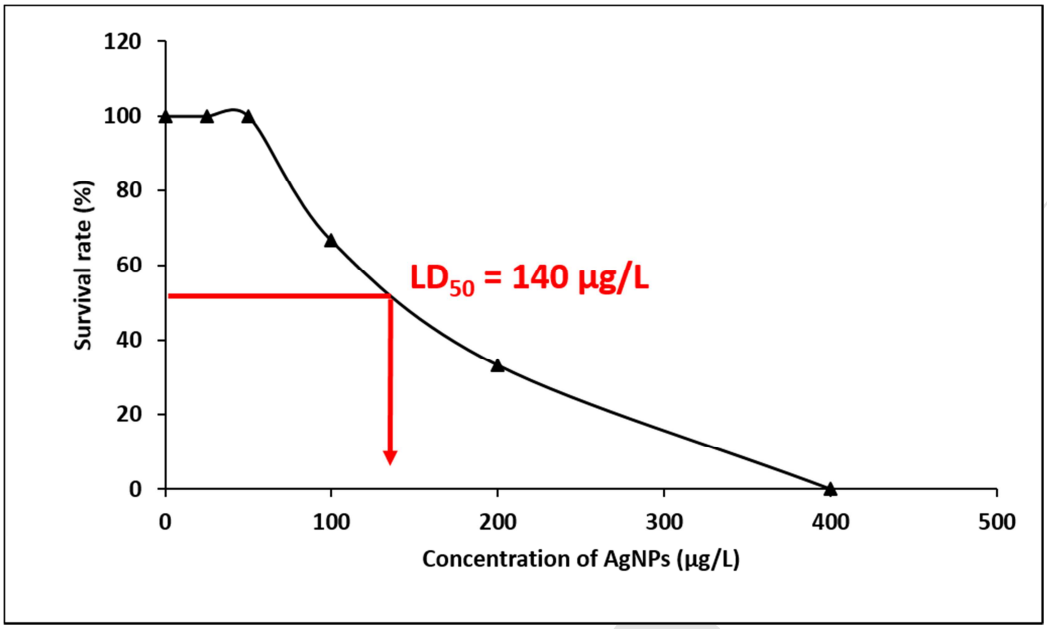

731

732

733 **Fig. S1.** Determination of toxicity levels of AgNPs to adult zebrafish. Fish were exposed to 0, 25,
734 50, 100, 200 and 400 µg/L of AgNPs (n = 10), and fish cumulative survival rate (%) was
735 calculated up to 96 hpi. The LD_{50} of AgNPs for the adult zebrafish was 140 µg/L.

736

Highlights

- Synthesized AgNPs at 50 µg/L were not toxic to zebrafish at 96 h post-immersion.
- AgNPs exhibited clear and faster closure of laser wounds on zebrafish.
- AgNPs immersion was more efficient than direct application for healing the wounds.
- AgNPs altered gene expression of inflammatory phases during wound healing.